TẠP CHÍ KHOA HỌC & CÔNG NGHỆ ĐẠI HỌC DUY TÂN
DTU Journal of Science and Technology 02(45) (2021) 109-116

TRƯỜNG ĐẠI HỌC DUY TÂN
DUYTAN UNIVERSITY

Using the Judd-Ofelt theory to analyze the lattice structure of the Dy^{+3} ions doped lithium-sodium aluminoborate glass

Sử dụng lý thuyết Judd-Ofelt để phân tích phổ về cấu trúc mạng của thủy tinh lithium-sodium aluminoborate glass pha tạp ion Dy^{+3}

Tran Ngoc[a,b*]
Trần Ngọc[a,b*]

[a]*Institute of Research and Development, Duy Tan University, Da Nang, 550000, Vietnam*
[a]*Viện Nghiên cứu và Phát triển Công nghệ Cao, Trường Đại học Duy Tân, Đà Nẵng*
[b]*Faculty of Natural Sciences, Duy Tan University, Da Nang, 550000, Vietnam*
[b]*Khoa Tự nhiên, Trường Đại học Duy Tân, Đà Nẵng*

(Ngày nhận bài: 23/3/2021, ngày phản biện xong: 10/4/2021, ngày chấp nhận đăng: 15/4/2021)

Abstract

Dy^{3+} doped lithium-sodium aluminoborate glass (60-x) B_2O_3-10Al_2O_3-15Na_2O-15Li_2O-xDy_2O_3 (ABLN: Dy^{3+}) are prepared by the conventional melting procedure. Optical absorption and luminescence spectra have been measured at room temperature. Using the Judd - Ofelt (JO) theory, the intensity parameters Ω_λ (λ = 2,4,6) have been evaluated for ABLN: Dy^{3+} glass. These intensity parameters are used to predict radiative properties that include electric (S_{ed}) magnetic (S_{md}) dipole line strength, radiative transition probabilities (A_R), lifetime (τ_R), branching ratios (β_R) for the excited levels of Dy^{3+}. In addition, the stimulated emission cross – sections ($\sigma_{\lambda p}$) have been predicted for the transitions $^4F_{9/2} \rightarrow {}^6H_J$ (J=15/2, 13/2, 9/2).

Keywords: Aluminoborate glasses; Judd-Ofelt theory; luminescence.

Tóm tắt

Thủy tinh lithium-sodium aluminoborate pha tạp Dy^{3+} (60-x) B_2O_3-10Al_2O_3-15Na_2O-15Li_2O-xDy_2O_3 (ABLN: Dy^{3+}) được chế tạo bằng phương pháp nung nóng chảy. Phổ hấp thụ và phổ huỳnh quang được đo tại nhiệt độ phòng. Sử dụng lý thuyết Judd – Ofelt (JO), các thông số cường độ Ω_λ (λ = 2, 4, 6) đã được xác định cho thủy tinh ABLN: Dy^{3+}. Các thông số cường độ này được sử dụng để dự đoán các đặc tính bức xạ bao gồm lực vạch lưỡng cực điện (S_{ed}), lưỡng cực từ (S_{md}), xác suất chuyển dời bức xạ (A_R), thời gian sống (τ_R), tỷ số phân nhánh (β_R) cho các mức kích thích của Dy^{3+}. Ngoài ra, tiết diện phát xạ ($\sigma_{\lambda p}$) đã được dự đoán cho quá trình các chuyển dời bức xạ: $^4F_{9/2} \rightarrow {}^6H_J$ (J=15/2,13/2,9/2).

Từ khóa: Thủy tinh aluminoborate; lý thuyết Judd-Ofelt; huỳnh quang.

[*] *Corresponding Author:* Tran Ngoc; Institute of Research and Development, Duy Tan University, Da Nang, 550000, Vietnam; Faculty of Natural Sciences, Duy Tan University, Da Nang, 550000, Vietnam
Email: daotaoqb@gmail.com

1. Introduction

Rare-earth (RE) ions doped borate glasses gained intensive attention from the researchers for various technological applications, such as solid-state lasers, optical fiber amplifiers, radiation dosimetry, high quality laser illuminators, white-LED (W-LEDs), and scintillators [1, 2, 3] etc. Borate glasses possess good RE ion solubility, high spectral transparency, low melting temperature, thermal stability and high mechanical stability, ease of synthesis, may be fabrication in different shapes and low manufacturing cost [2, 3, 4, 5]. Further, RE ions offer excellent emission efficiency because of their characteristic 4f–4f and 4f–5d transitions, and these 4f-4f transitions can give luminescence covering wide spectral range starting from ultraviolet (UV) to infrared (IR) as the 4f orbitals are very effectively protected from the interaction with external fields by $5s^2$ $5p^6$ shells [1, 3, 6]. However, high phonon energy (~1300–1500) cm^{-1} of borates increases the multi-phonon relaxation rates of the RE emission transitions, that decreases the luminescence and quantum efficiency. In the glass network, Al_2O_3 improves mechanical, chemical, electrical resistance and de-cluster RE dopant ions, which in turn enhance the emission efficiency by reducing the cross-relaxation (CR) losses [3, 7, 8, 9]. Depending on the concentration, Li_2O and Na_2O acts network modifier, causes improved stability, moisture resistance, transparency, and low rates of crystallization in the glasses [8, 10, 11]. Glass modifiers such as Li^+, Na^+ ions affect the physical and optical features, decrease viscosity and melting points of the glasses by disrupting the glass network and creating non-bridging oxygens [10, 11, 12, 13].

The visible luminescence of the Dy^{3+} ion mainly consists of yellow band at 570 - 600 nm corresponding to the $^4F_{9/2}$ - $^6H_{13/2}$ hypersensitive transition and the blue band at 470 - 500 nm corresponding to the $^4F_{9/2}$ - $^6H_{15/2}$ transition. Dysprosium doped glasses and crystals emit intense discrete radiation in the yellow (570 - 600 nm) and NIR (1,35 mm and 3,0 mm) regions that have potential technological applications in commercial displays and telecommunications [12, 13, 14]. The intensity of the $^4F_{9/2}$- $^6H_{13/2}$ hypersensitive transition strongly depends on the host, in contrast to a less sensitive $^4F_{9/2}$-$^6H_{15/2}$ transition of Dy^{3+} and results in different yellow to blue luminescence intensity ratios that largely change with concentration and/or glass composition.

In this work, we prepared and studied spectroscopic properties of Dy^{3+} ions in lithium-sodium aluminoborate glasses. Judd - Ofelt theory has been used to evaluate intensity parameters Ω_λ (λ = 2, 4, 6) by analyzing the absorption spectrum of ABLN: Dy^{3+} glass, and calculated the radiative transition probabilities, branching ratios, radiative lifetimes of $^4F_{9/2}$ excited level, stimulated emission cross - section for selected. Besides that, the potential application of the ABLN: Dy^{3+} glass as laser materials is described [15, 16, 17, 18, 19].

2. Experiment

Lithium-sodium aluminoborate glasses (ABLN glass) doped Dy^{3+} ions are prepared by conventional melt quenching technique. The molar composition of dysprosium doped ABLN glasses investigated in this work is (60-x) B_2O_3-10Al_2O_3-15Na_2O-15Li_2O-xDy_2O_3. High purity chemicals of B_2O_3, Na_2O, Li_2O, Al_2O_3 and Dy_2O_3 were used as starting materials. The batches were then placed in quartz cup and melted in an electrical furnace in air at 1323 K for 1.5 hours. The glasses were then annealed at 650 K for 2 hours. The glasses thus obtained were throughout, evenly, no bubble. The samples were cut out, grinding, polishing blocks rounded product size: thickness d = 1 mm,

radius r = 5 mm (used for the measurement of refractive index n, density, absorption and fluorescence); crushing and sorting grab particles range in size from 76 to 150 micron powder products (used for X-ray diffraction). The glass formation was confirmed by powder X-ray diffraction.

Optical absorption spectra were recorded in the wavelength regions 200 nm-2000 nm using Varian spectrometer system Cary 5E UV-VIS-NIR, with a resolution of 1 nm. Fluorescence and Excitation spectra were obtained at room temperature using Flourolog-3 Model FL3-22, Horiba JobinYvon resolution of 0.3 nm, excitation light xenon.

3. Results and discussion

3.1. Absorption spectra

Figure 1 show the absorption spectra of Dy^{3+} ions doped ABLN glass in the UV-Vis and NIR regions (from 300 nm to 1900 nm), respectively.

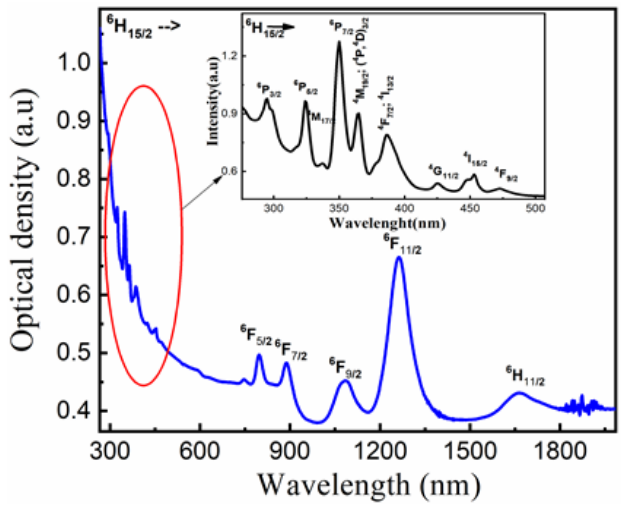

There are thirteen observed absorption peaks at 320, 350, 362, 381, 425, 455 and 470 nm in UV-Vis band (with fig are inserted in figure) and 745, 800, 895, 1090, 1270 and 1675 nm in near-infrared band, which are attributed to transitions from $^6H_{15/2}$ ground state to ($^6P_{3/2}$,$^4M_{17/2}$), $^6P_{7/2}$, ($^4M_{19/2}$,$^4(D,P)_{3/2}$), $^6P_{3/2}$, ($^4F_{7/2}$, $^4I_{13/2}$), $^4G_{11/2}$, $^4I_{15/2}$, $^4F_{9/2}$ and $^6F_{3/2}$, $^6F_{5/2}$, $^6F_{7/2}$, ($^6H_{7/2}$, $^6F_{9/2}$), ($^6H_{7/2}$, $^6F_{11/2}$), $^6H_{11/2}$ higher excited states in order of increasing wavelength, respectively. The transition from $^6H_{15/2}$ to the levels $^6H_{9/2}$ is hypersensitive in nature for Dy^{3+} ions which obeys the selection rule $|\Delta J| \leq 2$, $\Delta S = 0$ and $|\Delta L| \leq 2$ and any local structural change may sharply affect the position and intensity of this transition [6, 9, 13, 19, 21]. The energy of these absorption transitions of Dy^{3+} ions in ABLN glass host is also compared with Dy^{3+} diluted acid solution (aquo-ion) system and shown in Table 1.

Table 1: Energy transitions (v), bonding parameters (δ), the experimental (f_{exp}) and calculated (f_{cal}) oscillator strengths for ABLN: Dy^{3+} glass

Transition $^6H_{15/2}$ →	**v_c (cm^{-1})**	**v aquo (cm^{-1})**	**f_{exp} (×10^{-6})**	**f_{cal} (×10^{-6})**
$^6H_{11/2}$	5995	5850	3.21	3.07
$^6F_{11/2}$,$^6H_{9/2}$	7898	7730	16,54	16,57
$^6F_{9/2}$,$^6H_{7/2}$	9199	9100	5.97	6,50
$^6F_{7/2}$	11198	11000	4.91	5,15
$^6F_{5/2}$	12468	12400	3.25	2,36
$^6F_{3/2}$	13351	13250	0.39	0,48

$^4F_{9/2}$	21141	21100	0.54	0,39
$^4I_{15/2}$	22075	22100	1.18	1,04
$^4G_{11/2}$	23529	23400	0.29	0,21
$^4F_{7/2}$,$^4I_{13/2}$	25839	25800	4.45	1,91
$^4M_{19/2}$,$^4(D, P)_{3/2}$,$^6P_{3/2}$	27397	27400	3.90	3,50
$^6P_{7/2}$	28571	28550	9.12	7,89
$^6P_{3/2}$,$^4M_{17/2}$	30864	30892	3.14	2,02
$\bar{\beta} = 1.0063; \delta = -1.63$			rms = 1.09×10^{-6}	

Nephelauxetic effect- Bonding parameter

The bonding parameter (δ) is defined as $\delta = \left[\left(1-\bar{\beta}\right)/\bar{\beta}\right]\times 100$ [1, 4, 5], where $\bar{\beta} = (\sum \beta)/n$ and nephelauxetic ratio $\beta = \nu_c/\nu_a$, (ν_c and ν_a are energies of the corresponding transitions in the complex and aquo-ion, respectively, and n to refers to the number of levels that are used to compute $\bar{\beta}$ values) [1, 2]. Depending on the field environmental, the bonding parameter (δ) can be received the positive or negative value indicating covalent or ionic bonding. In our sample, the values of $\bar{\beta}$ and δ bonding parameter are 1.0063 and -1.63, respectively. Thus, the bonding of Dy^{3+} ions with the local host is ionic bonding [17, 19, 20].

Oscillator strengths and JO parameters

The experimental (f_{exp}) and calculation oscillator strengths (f_{cal}) of absorption bands are determined using Eq [15, 16, 18]:

$$f_{exp} = 4{,}318.10^{-9}\int \alpha(\nu)d\nu \quad (1)$$

$$f_{cal} = \frac{8\pi^2 mc}{3h\bar{\lambda}(2J+1)} n\left(\frac{n^2+2}{3n}\right)^2 \sum_{\lambda}\Omega_{\lambda}\left\|U^{(\lambda)}\right\|^2 \quad (2)$$

where α is molar extinction coefficient at energy ν (cm^{-1}). The $\alpha(\nu)$ values can be calculated from absorbance A by using Lambert – Beer's law: $A = \alpha(\nu)Cd$, C is concentration [dim: L^{-3}; units: mol^{-1}], d is the optical path length [dim: L; units: cm]. n is the refractive index of the material, J is the total angular momentum of the ground state, Ω_λ are the JO intensity parameters and $\left\|U^{\lambda}\right\|^2$ are the squared doubly reduced matrix of the unit tensor operator of the rank λ = 2, 4, 6 is calculated from intermediate coupling approximation for a transition $|\psi J\rangle \rightarrow |\psi' J'\rangle$. These reduced matrix elements did not nearly depend on host matrix as noticed from earlier studies [15, 17]. All thirteen absorption bands have been analyzed using JO theory and were least squared fitted to yield the best fit values for the JO parameters. The results of the parameters a, b, c, for the transitions of Dy in the glass ABLN are: Ω_2 = $16{,}30\times10^{-20} \pm 0.82\times10^{-20}$ cm^2, Ω_4 = $5{,}81\times10^{-20} \pm 0.77\times10^{-20}$ cm^2, Ω_6 = $5.28\times10^{-20} \pm 0.48\times10^{-20}$ cm^2. Table 2 compared the JO intensity parameters obtained for ABLN: Dy^{3+} glass with some of the reports on systems: Dy^{3+} [15 - 22].

Table 2: The JO parameters of Dy^{3+} ions doped various hosts

Host matrix	$\Omega_2(\times10^{-20}cm^2)$	$\Omega_4(\times10^{-20}cm^2)$	$\Omega_6(\times10^{-20}cm^2)$	Ω_4/Ω_6	Ref.
ABLN: Dy^{3+} glass	**16,30**	**5,81**	**5.28**	**1,10**	**Present**
LYB: Dy^{3+} glass	12,83	3,47	3,43	1,01	[7]
PKBFA: Dy^{3+} glass	10,41	2,29	2,07	1,10	[21]
NaLTB: Dy^{3+} glass	9,86	3,39	2,41	1,41	[20]
NaLTB: Dy^{3+} glass	9,25	2,87	2,29	1,25	[22]
LiLTB: Dy^{3+} glass	8,75	2,62	2,07	1,26	[22]
PKMAF: Dy^{3+} glass	7,04	1,73	1,57	1,10	[21]

The Table 2 shows the values of Ω_2 and Ω_6 in ABLN glass are larger than those of the different hosts. The characteristic feature of the Ω_2 is that it is sensitive to the local environment of the RE^{3+} ions and is often related with the asymmetry of the coordination structure, polarizability of ligand ions or molecules and bonding nature [15, 16, 19, 23, 24]. The larger of Ω_2 parameter in ABLN: Dy^{3+} glass than other hosts can be attributed to lower symmetry of the coordination structure surrounding the RE^{3+} ion. The Ω_6 parameter related to the rigidity of the medium in which the RE^{3+} ions are embedded. Rigid matrices show low values for the Ω_6 parameter [15, 18]. The larger of Ω_6 parameter in ABLN: Dy^{3+} glass than other hosts suggests that the rigidity of the surrounding environment Dy^{3+} in ABLN glass is lower than other hosts. The spectroscopic quality factor $\chi = \Omega_4/\Omega_6$, is one of the ABLN important lasing characteristic parameters which is used to predict the stimulated emission in any active medium. The Dy^{3+} doped glass hosts possessing spectroscopic quality factors in the range 0.42–1.92 are the good candidates for laser active media [12, 13, 14, 19]. The observed value of χ in ABLN: Dy^{3+} glass is 1.10, which suggests that ABLN: Dy^{3+} glass is good material for various optical devices.

3.2. Fluorescence spectra and radiation properties

From the JO parameters, the radiative properties such as the electric (S_{ed}) and magnetic (S_{md}) dipole line strengths, the radiative transition rates (A_R), radiative lifetime (τ_R), branching ratios (β_R) were calculated for excited levels $^4F_{9/2}$. The results are showed in Table 3.

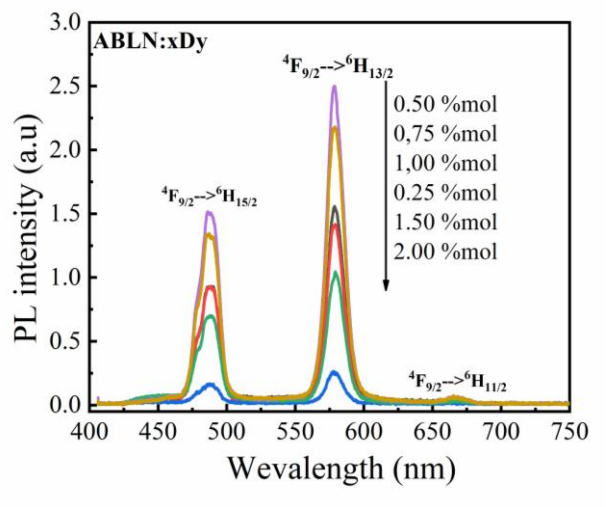

Fig. 2. The emission spectrum of ABLN: Dy^{3+} glass under excitation by 365 nm

As shown in Fig. 2, which illustrates the emission spectrum using the 365 nm excitation wavelength of xenon lamp source, 4 emission bands at 481, 575, 664 and 755 nm which are attributed to transitions from $^4F_{9/2}$ to $^6H_{15/2}$, $^6H_{13/2}$, $^6H_{11/2}$ and $^6H_{9/2}$ and states, respectively, of Dy^{3+}ions. But among of them, the yellow (Y) band (575 nm) corresponds to the hypersensitive transition $^4F_{9/2} \rightarrow {}^6H_{13/2}$, and the blue (B) band (481 nm) corresponds to the $^4F_{9/2} \rightarrow {}^6H_{15/2}$ transition are the dominant bands in the emission spectrum. The intensity ratio of yellow emission to blue emission (Y/B) of the Dy^{3+}ions dependents on the asymmetry of the ligand. With the ABLN: Dy^{3+}, the Y/B ratio is 1.27 and higher than other hosts [19-21]. The higher value of Y/B indicates that the higher degree of covalence between dysprosium and oxygen ions. From the JO parameters and refractive index, the radiative properties such as the electric (S_{ed}) and magnetic (S_{md}) dipole line strengths, the radiative transition rates (A_R), radiative lifetime (τ_R), branching ratios (β_R) were calculated for $^4F_{9/2}$ excited levels. The results are showed in table 3.

Table 3. Transition energies (ν), radiative transition probabilities (S_{ed}, S_{md}, A and A_T), radiative lifetime (ι_R) and branching ratios (β_R) for excited levels.

SLJ	*S'L'J'*	ν (cm^{-1})	S_{ed} (cm^2)	S_{md} (cm^2)	A (s^{-1})	β_R (%)
$^4F_{9/2}$	$^6F_{1/2}$	7,296	4.90E-42	0.00E+00	1.94E-01	8.01E-03
	$^6F_{3/2}$	7,908	4.00E-42	0.00E+00	1.97E-01	8.16E-03
	$^6F_{5/2}$	8,552	2.59E-42	0.00E+00	1.71E+01	7.09E-01
	$^6F_{7/2}$	9,944	1.03E-41	4.00E-41	1.13E+01	4.67E-01
	$^6H_{5/2}$	10,901	6.13E-40	0.00E+00	8.11E+00	3.35E-01
	$^6H_{7/2}$	11,962	2.30E-40	1.76E-41	4.06E+01	1.68E+00
	$^6F_{9/2}$	12,065	1.07E-41	1.59E-41	1.94E+01	8.01E-01
	$^6F_{11/2}$	13,257	2.09E-40	2.26E-42	5.10E+01	2.11E+00
	$^6H_{9/2}$	13,398	1.61E-41	1.65E-40	4.46E+01	1.84E+00
	$^6H_{11/2}$	15,209	4.34E-40	3.13E-41	1.59E+02	6.59E+00
	$^6H_{13/2}$	17,628	2.89E-39	0.00E+00	1.62E+03	6.69E+01
	$^6H_{15/2}$	21,182	4.64E-40	0.00E+00	4.48E+02	1.85E+01
$A_{T(4F9/2)} = 2423\ s^{-1}$; $\tau_{R(4F9/2)} = 414\ \mu s$						

From the emission spectrum of ABLN: Dy^{3+} glass, the emission peak positions (λ_p), effective line width ($\Delta\lambda_{eff}$), measured branching ratios (β_{exp}), stimulated emission cross – section $\sigma(\lambda_P)$ and integrated emission cross – section (Σ_{if}) to have calculated for $^4F_{9/2} \rightarrow {}^6H_J$ (J = 15/2, 13/2, 11/2, 9/2) transitions. The results are displayed in Table 4.

Table 4. Emission peak positions (λ_p), effective line width ($\Delta\lambda_{eff}$), radiative transition probabilities (A), branching ratios (β_{exp}), stimulated emission cross – section $\sigma(\lambda_P)$ and integrated emission cross – section (Σ_{if}) for $^4F_{9/2} \rightarrow {}^6H_J$ transitions of Dy^{3+} in ABLN glass.

$^4F_{9/2}$ →	λ_p (nm)	$\Delta\lambda_{eff}$ (nm)	A (s^{-1})	$\sigma(\lambda_p)$ ($\times 10^{-22}$ cm^2)	Σ_{if} ($\times 10^{-18}$ cm)	β_R (%)	
						exp	cal
$^6H_{11/2}$	661.3	26.1	160	6,52	0,39	4,62	6,59
$^6H_{13/2}$	570.7	16.3	1626	59,8	2,99	56,32	66,80
$^6H_{15/2}$	480.4	18.7	450	7,26	0,62	40,63	18,53

In general, the luminescence branching ratio is a critical parameter to the laser designer, because it characterizes the possibility of attaining stimulated emission from any specific transition. In this work, the predicted branching ratio of $^4F_{9/2} \rightarrow {}^6H_{13/2}$ transition get a maximum value and be 66,8 %, while that the measured ratio is 56.32 %. Thus, there is a good agreement between experimental and calculated branching ratios [19].

The integrated emission cross–section, Σ_{if}, was an important parameter when considering the laser emission of the material. When the integrated emission cross–section is greater than 10^{-18} cm, laser emission is probable [13]. In our case, with the $^4F_{9/2} \rightarrow {}^6H_{13/2}$ transition, the integrated emission cross – section is 2.99×10^{-18} cm. The stimulated emission cross – section $\sigma(\lambda_P)$, which is an another of the most important parameter that affects the potential laser performance and its value signifies rate of energy extraction from the lasing material. It is found that $^4F_{9/2} \rightarrow {}^6H_{13/2}$ transition exhibits maximum $\sigma(\lambda_P)$ ($59,8\times10^{-22}cm^2$). The large values of branching ratio, integrated emission cross – section and stimulated emission cross section suggest that the $^4F_{9/2} \rightarrow {}^6H_{13/2}$ transition can give rise to lasing action.

4. Conclusion

Dy^{3+}doped lithium-sodium aluminoborate glasses were prepared by melt quenching technique and investigated through the absorption and photoluminescence spectra. The negative value of bonding parameter δ shows that the bonding of Dy^{3+} ions with the local host is ionic bonding. JO theory has been applied to determine the intensity parameters by analyzing the absorption spectra. The larger of Ω_2 parameter and Y/B ratio in ABLN: Dy^{3+} glass than other hosts can be attributed to lower symmetry of the coordination structure surrounding the RE^{3+} ion. The large of the spectroscopic quality (χ) suggests that ABLN: Dy^{3+} glass is good material for various optical devices. The large values of branching ratio, integrated emission cross – section and stimulated emission cross section suggest that the $^4F_{9/2} \rightarrow {}^6H_{13/2}$ transition can give rise to lasing action.

References

[1] Christane Görller, Walrand and K. Binnemans (1998), *Spectral intensities of f – f transition*, Handbook on the Physics and Chemistry of Rare Earths. Vol.25, pp 101 – 252.

[2] Carnall W.T., Fields P.R., and Rajnak K (1968), *Electronic Energy Levels in the Trivalent Lanthanide Aquo Ions. I. Pr^{3+}, Nd^{3+}, Pm^{3+}, Sm^{3+}, Dy^{3+}, Ho^{3+}, Er^{3+}, and Tm^{3+}*, J. Chem. Phys, 49, 10, 4424-4442.

[3] P.P. Pawar, S.R. Munishwar, S. Gautam, R.S. Gedam (2017), *Physical, thermal, structural and optical properties of Dy^{3+} doped lithium alumino-borate glasses for bright W-LED*, J. Lumin. 183 79-88.

[4] P.V. Do, T. Ngoc, N.X. Ca, L. D. Thanh, P. T. T. Nga, T. T. C. Thuy, N. V. Nghia (2021), *Study of spectroscopy of Eu^{3+} and energy transfer from Ce^{3+} to Eu^{3+} in sodium-zinc-lead-borate glass*, Journal of Luminescence, 229, 117660. https://doi.org/10.1016/j.jlumin.2020.117660

[5] P.V. Do, V.P.Tuyen, V.X. Quang, L. X.Hung, L.D. Thanh, T. Ngoc, N. V. Tam (2016),; *Investigation of spectroscopy and the dual energy transfer mechanisms of Sm^{3+} doped telluroborate glasses*, Optical Materials, 55-62-67. https://doi.org/10.1016/j.optmat.2021.03.023

[6] J. Pisarska (2009), *Optical properties of lead borate glasses containing Dy^{3+} ions*, J. Phys. Condens. Matter 21, 285101/1–6.

[7] E. Kaewnuam, N. Wantana, H.J. Kim, J. Kaewkhao (2017), *Development of lithium yttrium borate glass doped with Dy^{3+} for laser medium, W-LEDs and scintillation materials applications*, J. Non-Cryst. Solids 464, 96–103.

[8] H.H. Xiong, L.F. Shen, E.Y.B. Pun, H. Lin (2014), *High-efficiency fluorescence radiation of Dy^{3+} in alkaline earth borate glasses*, J. Lumin. 153, 227–232.

[9] Tripathi G, Rai VK, Rai SB, *Spectroscopy and upconversion of Dy^{3+} doped in sodium zinc phosphate glass*, Spectrochim Acta A 2005;62:1120–4.

[10] Tanabe S, Kang J, Hanada T, Soga N (1998), *Yellow/blue luminescences of Dy^{3+}doped borate glasses and their anomalous temperature variations*, J Non-Cryst Solids, 239:170–5.

[11] S.A. Saleema, B.C. Jamalaiah, M. Jayasimhadri, A. Srinivasa Rao,Kiwan Jang, L. Rama Moorthy (2011), *Luminescent studies of Dy3+ ion in alkali lead tellurofluoroborate glasses*; Journal of Quantitative Spectroscopy & Radiative Transfer, pp. 78–84.

[12] Surendra Babu S, Babu P, Jayasankar CK, Siewers W, Wortmann G (2011), *Optical spectroscopy of Dy^{3+}: phosphate and fluorophosphates glasses*. Opt Mater, 31, 624–31.

[13] Sardar DK, Bradley WM, Yow RM, Gruber JB, Zandi B (2004), *Optical transitions and absorption intensities of Dy^{3+} (4f9) in YSGG laser host*. J Lumin, 106:195–203.

[14] Yang Z, Li B, He F, Luo L, Chen W (2008), *Concentration dependence of Dy^{3+}1.3 mm luminescence in Ge–Ga–Sb–Se glasses.* J Non-Cryst Solids, 354:1198–200.

[15] Judd BR (1962), *Optical absorption intensities of rare earth ions*, Phy Rev, 127:750–61.

[16] Jørgensen CK, Reisfeld R (1983). *Judd–Ofelt parameters and chemical bonding*. J Less-Common Met. 93,107–12.

[17]. Wang D., Guo Y., Wang Q., Chang Z., Liu J., Luo J (2009), Judd-Ofelt analysis of spectroscopic properties of Tm^{3+} in K_2YF_5 , Journal of Alloys and Compounds, 474, 1–2, 23-25

[18] Ofelt GS (1962). *Intensities of crystal spectra of rare-earth ions*. J Chem Phys, 37, 511–20.

[19] Vu Phi Tuyen, Vu Xuan Quang, Phan Van Do, Luong Duy Thanh, Nguyen Xuan Ca, Vu Xuan Hoa, Le van Tuat, Le Anh Thi, Masayuki Nogamia (2019), *An in-depth study of the Judd-Ofelt analysis, spectroscopic properties and energy transfer of Dy^{3+} in alumino-lithium-telluroborate glasses*, Journal of Luminescence, 210-435-443, https://doi.org/10.1016/j.jlumin.2019.03.009.

[20] Do Van Phan, Vu Xuan Quang, Ho Van Tuyen, Tran Ngoc, Vu Phi Tuyen, Luong Duy Thanh, Nguyen Xuan Ca, Nguyen Thi Hien (2019), *Structure, optical properties and energy transfer in potassium-alumino borotellurite glasses doped with Eu^{3+} ions*, Journal of Luminescence, 216,116748. https://doi.org/10.1016/j.jlumin.2019.116748

[21] X.M. Zang, D.S. Li, E.Y.B. Pun, H. Lin (2017), *Dy^{3+} doped borate glasses for laser illumination*, Opt. Mater. Express 7, 2040–2054.

[22] B.M. Saisudha, H.G. Ooi, S.K. Ferrell, P.K. Babu (2017), *Effect of metal and semiconducting nanoparticles on the optical properties of Dy^{3+} ions in lead borate glasses*, Mater.Res. Bull. 92 52–64.

[23] G. Lakshminarayana, S.O. Baki, A. Lira, I.V. Kityk, U. Caldiño, K.M. Kaky, M.A. Mahdi (2017), *Structural, thermal and optical investigations of Dy^{3+}-doped B_2O_3–WO_3–ZnO–Li_2O–Na_2O glasses for warm white light emitting applications*, J.Lumin. 186, 283–300.

crystal, J. Alloy. Compd 474 (2009) 23-25.

[24] Lin H, Pun EYB, Wang X, Lin X (2005). *Intense visible fluorescence and energy transfer in Dy^{3+}, Tb^{3+}, $Sm^{3+}$and Eu^{3+}doped rare-earth borate glasses*. J Alloys Compd, 390,197–201.